

## Fusion and planarization of a quinoidal porphyrin dimer†

Iain M. Blake, Alexander Krivokapic, Martin Katterle and Harry L. Anderson\*

Department of Chemistry, University of Oxford, Dyson Perrins Laboratory, South Parks Road, Oxford, UK OX1 3QY. E-mail: harry.anderson@chem.ox.ac.uk

Received (in Cambridge, UK) 7th May 2002, Accepted 21st June 2002

First published as an Advance Article on the web 8th July 2002

The crystal structure, near-infrared spectrum and electrochemistry of a quinoidal triply-linked porphyrin dimer are compared with those of its singly-linked precursor; fusing the two porphyrins planarizes the  $\pi$ -system and reduces the optical HOMO–LUMO gap while increasing the gap between the first oxidation and reduction potentials.

Near infrared (NIR) radiation has many important technological applications,<sup>1</sup> and there is a need for new optoelectronic materials operating in this wavelength region (800–2000 nm). Conjugated porphyrin oligomers<sup>2–5</sup> are promising materials in this context, and recently two strategies have been developed for shifting their absorption spectra far into the NIR: we have synthesized strongly conjugated quinoidal porphyrin dimers,<sup>3</sup> while Osuka and coworkers have created directly fused porphyrin tapes with *meso*–*meso*-,  $\beta$ – $\beta$ - and  $\beta$ – $\beta$ -links.<sup>4,5</sup> Here we discuss the synthesis, electronic structure and crystal structure of a porphyrin dimer **1** which simultaneously exemplifies both these design strategies.

Previously we reported the synthesis of quinoidal porphyrin dimer **2** from dibromo dimer **3** as shown in Scheme 1.<sup>3</sup> Steric repulsion between the inner  $\beta$ -hydrogens forces this molecule into a non-planar conformation. The <sup>1</sup>H and <sup>13</sup>C NMR spectra of **2** show that the two porphyrin macrocycles are not coplanar, but do not allow one to distinguish between the two possible non-planar geometries ( $D_2$  twist or  $C_{2h}$  double fold). Molecular mechanics calculations predicted a twisted  $D_2$  conformation, however single crystal X-ray diffraction has now revealed that the molecule has the alternative  $C_{2h}$  conformation in the solid state, as shown in Fig. 1.‡ This is the structure of the pyridine complex, with one molecule of pyridine coordinated to each zinc atom. The molecule has a crystallographic inversion centre

and there is almost a plane of symmetry through both zinc atoms, perpendicular to both macrocycles, giving the molecule virtual  $C_{2h}$  symmetry. The central  $C_{\text{meso}}=C_{\text{meso}}$  bond length is 1.38 Å, and the tetra-substituted alkene unit is planar (maximum deviation  $\pm 0.03$  Å for six carbon atoms). The mean planes of the two macrocycles are parallel, with a separation of 2.79 Å, and the two  $\pi$ -systems almost overlap, with a  $\beta$ -C... $\beta$ -C inter-macrocycle distance of 3.05 Å. The ends of the molecule are distorted to minimize steric interaction between the nitrile groups and the outer  $\beta$ -hydrogens, as observed in related structures.<sup>3,6</sup>

The non-planar conformation of **2** probably disrupts the conjugation, so we sought to fuse and planarize the molecule by removing the four central hydrogens, to give compound **1**. We explored both routes shown in Scheme 1. Oxidation of dibromo-dimer **3** under Osuka's scandium(III) triflate/DDQ conditions<sup>5</sup> gave the fused dibromo-dimer **4**, but in low yield (9%) due to incomplete reaction (45% of **3** was reisolated). Quinoidalization of **4** using Takahashi coupling conditions<sup>3,6</sup> proceeded smoothly to give the target compound **1** in 84% yield. Surprisingly, oxidation of the quinoidal dimer **2** worked much better than oxidation of **3**, giving **1** in 83% yield. The strain in

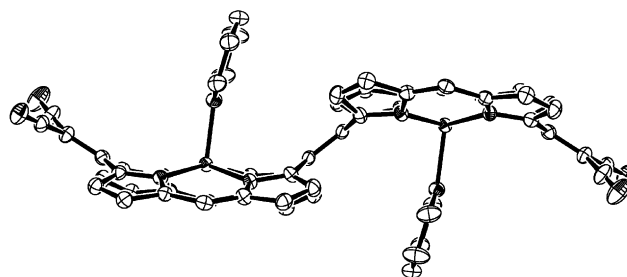
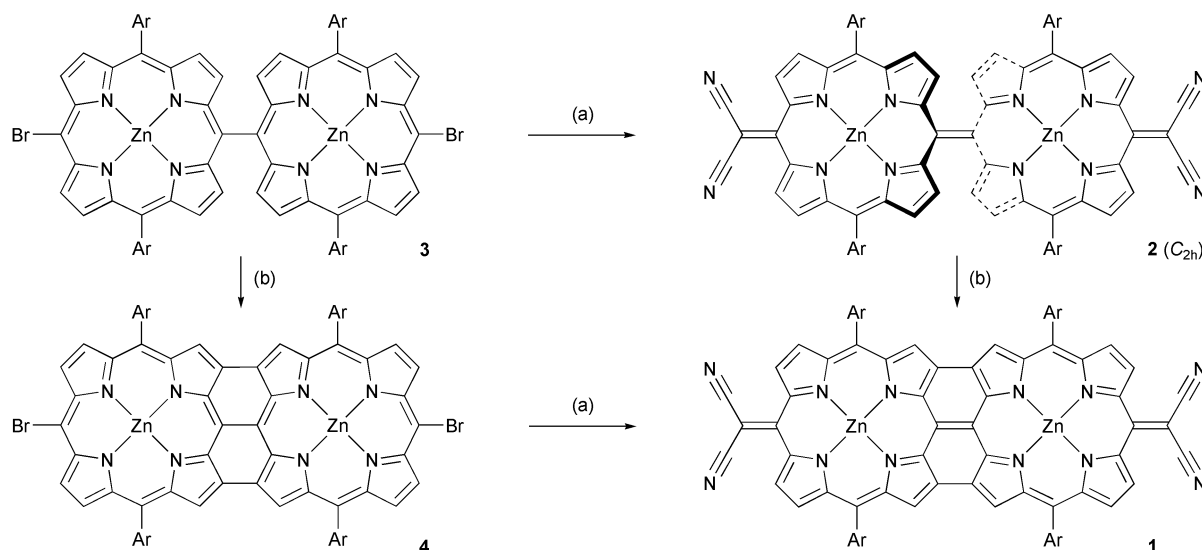
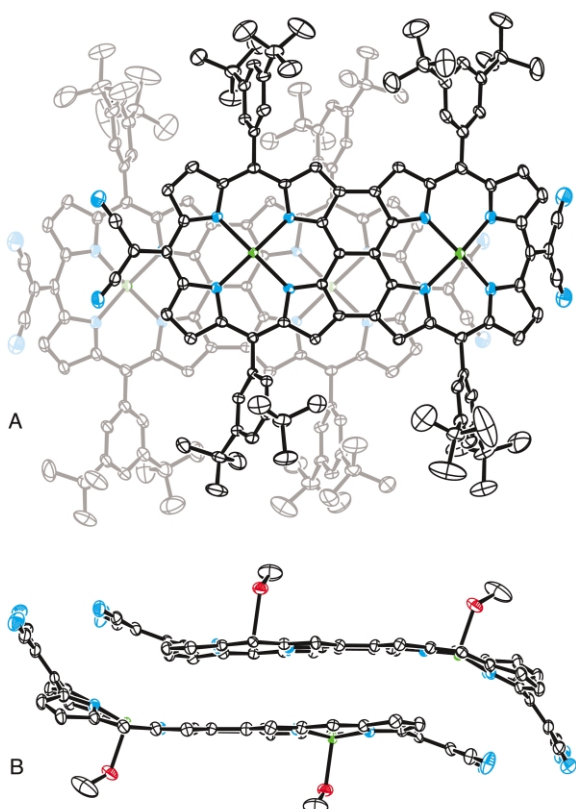


Fig. 1 Side view of the structure of 2-(pyridine)<sub>2</sub> omitting aryl substituents (50% probability ellipsoids).



Scheme 1 Reagents: (a) NaCH(CN)<sub>2</sub>, [Pd<sub>2</sub>(dba)<sub>3</sub>], CuI, PPh<sub>3</sub> then NIS, (b) Sc(OTf)<sub>3</sub>, DDQ. (Ar = 3,5-Bu<sub>2</sub>C<sub>6</sub>H<sub>3</sub>).

† Electronic supplementary information (ESI) available: synthetic procedures. See <http://www.rsc.org/suppdata/cc/b2/b204265g/>



**Fig. 2** Two views of the structure of **1**·(MeOH)<sub>2</sub>, (A) omitting methanol and (B) omitting aryl substituents (50% probability ellipsoids).

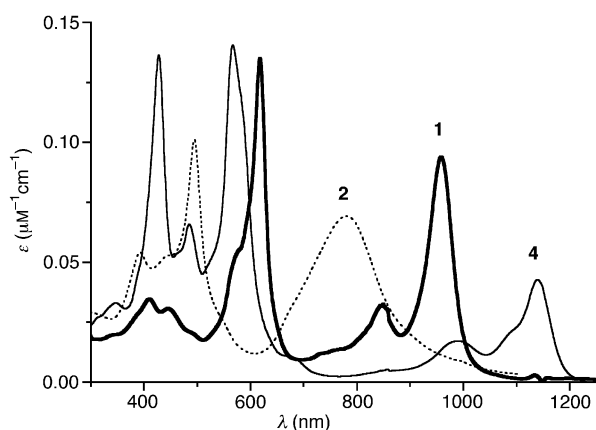


**Fig. 3** Absorption spectra of **1**, **2** and **4** in 1% C<sub>5</sub>H<sub>5</sub>N–CH<sub>2</sub>Cl<sub>2</sub>.

**2** apparently facilitates its oxidation, making this the best route to **1**.

The crystal structure of the methanol complex of **1** is shown in Fig. 2.‡ This compound crystallizes as a tight bimolecular aggregate; the two molecules in each aggregate are related *via* an inversion centre. The 'naphthalene' core of the dimer is planar to within ±0.04 Å. The central C<sub>meso</sub>–C<sub>meso</sub> bond length is 1.43 Å, and although this is formally a double bond it is not significantly shorter than the formally single C<sub>meso</sub>–C<sub>meso</sub> bonds in Osuka's triply linked dimers (analogs of **4** with aryl instead of bromine substituents).<sup>4</sup> The plane-plane separation at the centre of the aggregate is 3.4 Å and the closest intermolecular contact is between a nitrile nitrogen and the central carbon of the dicyanomethylene unit (N⋯C distance = 3.13 Å).

The electronic absorption spectra of dimers **1**, **2** and **4** are compared in Fig. 3. As expected, the absorption of **1** ( $\lambda_{\max} = 958$  nm;  $\epsilon = 9.4 \times 10^4$  M<sup>-1</sup>cm<sup>-1</sup>) is sharper and more red-shifted than that of **2** ( $\lambda_{\max} = 780$  nm;  $\epsilon = 6.9 \times 10^4$  M<sup>-1</sup>cm<sup>-1</sup>), but it is surprising that dimer **4** exhibits the longest

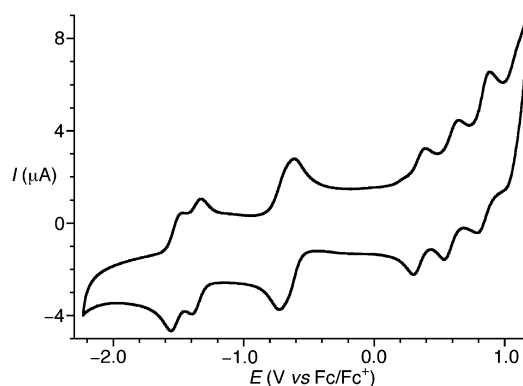


**Fig. 4** Cyclic voltammogram of **1**.§

wavelength absorption ( $\lambda_{\max} = 1139$  nm;  $\epsilon = 1.1 \times 10^4$  M<sup>-1</sup>cm<sup>-1</sup>). The unexpected blue shift on quinoidalization of **4** to **1** might be due to the greater bond-length alternation in quinoidalized porphyrins.

While planarization of **2** to **1** results in a dramatic decrease in the optical HOMO–LUMO gap, the electrochemical gap between the first oxidation and reduction potentials ( $E_1^{\text{Ox}} - E_1^{\text{Red}}$ ) increases from 0.53 to 1.00 V on conversion of **2** to **1**. Compound **1** displays reversible oxidation ( $E_1^{\text{Ox}} = 0.35$  V) and reduction ( $E_1^{\text{Red}} = -0.65$  V) waves, whereas the redox processes of **2** are poorly reversible, but can be measured by square wave voltammetry ( $E_1^{\text{Ox}} = 0.10$  V;  $E_1^{\text{Red}} = -0.43$  V).§ The easier oxidation and reduction of **2** probably reflects the strain in the neutral form which would be released if oxidation or reduction converts the central C=C link to a single bond, allowing the macrocycles to twist to orthogonal orientations. The first and second one-electron oxidations of **1** are separated by 0.25 V, whereas the first and second one-electron reductions almost coincide as seen in Fig. 4.

We thank EPSRC, DSTL and EOARD for supporting this work, the EPSRC Mass Spectrometry Service (Swansea) for mass spectra, and Dr K. J. McEwan (DSTL, Malvern) for recording NIR spectra.

## Notes and references

‡ *Crystal data* for **1**: crystals grown from CHCl<sub>3</sub>–CH<sub>3</sub>OH, C<sub>102</sub>H<sub>96</sub>N<sub>12</sub>Zn<sub>2</sub>·8CH<sub>4</sub>O·3H<sub>2</sub>O,  $M = 1931.13$ , triclinic, space group  $P\bar{1}$ ,  $a = 14.6863(2)$ ,  $b = 17.3636(2)$ ,  $c = 22.3909(3)$  Å,  $\alpha = 110.2640(4)$ ,  $\beta = 98.4021(4)$ ,  $\gamma = 96.5091(9)^\circ$ ;  $V = 5215.6$  Å<sup>3</sup>,  $Z = 2$ ,  $\mu = 0.524$  mm<sup>-1</sup>,  $R = 0.0648$ ,  $R_w = 0.0676$ ,  $I_o = 13933$  observed [ $I > 3.0\sigma(I)$ ] reflections out of  $N = 19263$  unique, GOF = 1.0537.

*Crystal data* for **2**: crystals grown from CHCl<sub>3</sub>–pyridine–pentane, C<sub>102</sub>H<sub>100</sub>N<sub>12</sub>Zn<sub>2</sub>·2C<sub>5</sub>H<sub>5</sub>N·4CHCl<sub>3</sub>,  $M = 2260.49$ , triclinic, space group  $P\bar{1}$ ,  $a = 14.4288(3)$ ,  $b = 15.0483(3)$ ,  $c = 15.3810(4)$  Å,  $\alpha = 82.9828(7)$ ,  $\beta = 73.3295(7)$ ,  $\gamma = 63.312(1)^\circ$ ;  $V = 2858.4$  Å<sup>3</sup>,  $Z = 1$ ,  $\mu = 0.753$  mm<sup>-1</sup>,  $R = 0.0534$ ,  $R_w = 0.0645$ ,  $I_o = 6723$  observed [ $I > 3.0\sigma(I)$ ] reflections out of  $N = 10015$  unique, GOF = 1.0480.

Both data sets were collected on an Enraf Nonius Kappa CCD diffractometer;  $T = 150$  K,  $\lambda(\text{Mo-K}\alpha) = 0.71073$  Å. CCDC reference numbers 185524 and 185525. See <http://www.rsc.org/suppdata/cc/b2/b204265g/> for crystallographic data in CIF or other electronic format.

§ Redox potentials were measured by square wave and cyclic voltammetry (0.1 V s<sup>-1</sup>) in CH<sub>2</sub>Cl<sub>2</sub> with 0.1 M Bu<sub>4</sub>NPF<sub>6</sub> and a carbon working electrode, and are quoted relative to  $E_1^{\text{Ox}}$  of internal ferrocene.

- J. Fabian, H. Nakazumi and M. Matsuoka, *Chem. Rev.*, 1992, **92**, 1197.
- H. L. Anderson, *Chem. Commun.*, 1999, 2323; M. G. Vicente, L. Jaquinod and K. M. Smith, *Chem. Commun.*, 1999, 1771.
- I. M. Blake, L. H. Rees, T. D. W. Claridge and H. L. Anderson, *Angew. Chem., Int. Ed.*, 2000, **39**, 1818.
- A. Tsuda, H. Furuta and A. Osuka, *J. Am. Chem. Soc.*, 2001, **123**, 10304.
- A. Tsuda and A. Osuka, *Science*, 2001, **293**, 79.
- I. M. Blake, H. L. Anderson, D. Beljonne, J.-L. Brédas and W. Clegg, *J. Am. Chem. Soc.*, 1998, **120**, 10764.